RSC Advances

PAPER

View Article Online
View Journal | View Issue

Cite this: *RSC Adv.*, 2025, **15**, 36152

Design, synthesis and anticancer evaluation of naphthalen-1-yloxyacetamide derivatives against MCF-7 cells

Maha Ali Alghamdi,[a] Mustafa R. Abdulbaqi,[b] Rana Abdullah Alghamdi,[cd] Eman Fayad,[a] Dalal Nasser Binjawhar,[e] Hanadi A. Katouah,[f] Abdullah Yahya Abdullah Alzahrani [g] and Amal M. Youssef Moustafa*[h]

Herein, a set of naphthalen-1-yloxyacetamide-tethered 2,3-disubstituted acrylamide conjugates was synthesized in a good yield *via* the reaction of naphthalene-1-yloxyacetohydrazide and an equimolar amount of respective ethyl 2,3-disubstituted acrylate ester in pure ethanol with a catalytic base of fused sodium acetate. All conjugates were assessed for their anti-proliferative activity against the MCF-7 *Br Ca* cell line. The results found that conjugate **5d** with 3-(4-methoxyphenyl)-2-phenylacrylamide attached to the naphthalen-1-yloxyacetamide moiety demonstrated potent cytotoxic activity against the investigated MCF-7 *Br Ca* cells. Thereafter, compounds **5c**, **5d**, and **5e** were subsequently evaluated for their aromatase inhibitory activity. Moreover, the representative promising conjugate in cytotoxic and aromatase inhibition assays was tested to investigate its impact on the cell cycle analysis and apoptosis promotion with the aim to get more insight into the antitumor mechanism of action of the target naphthalen-1-yloxyacetamide-acrylamide conjugates. In the examined MCF-7 cells, compound **5d** heightened cell cycle arrest during the G1 phase and provoked cellular apoptosis. Furthermore, compound **5d** increased the apoptosis percentage *via* the expressive downregulation of the anti-apoptotic protein Bcl-2 and the upregulation of Bax and caspase 9 levels relative to untreated groups.

Received 31st August 2025
Accepted 20th September 2025

DOI: 10.1039/d5ra06524k

rsc.li/rsc-advances

1. Introduction

Breast cancer (*Br Ca*) is the second most frequent cancer worldwide and the fifth leading cause of cancer-related death.[1] It is the leading cause of cancer-related deaths among women in less developed regions, and the second leading incidence in more developed areas, behind lung cancer.[2] High levels of estrogen have been noted to increase the risk of developing breast malignancy, especially in the estrogen receptor-positive (ER+) subtype, which is the subtype diagnosed in 70% of cases.[3] It was reported that estrogen facilitates growth and proliferation of several *Br Ca* cell types (*i.e.*, estrogen-dependent mammary carcinoma cells (MCF-7)).[4] Drugs that limit the synthesis of estrogens or inhibit estrogen receptor (ER) continue to be the mainstay of *Br Ca* treatment and management.[5,6] Aromatase is expressed in a variety of tissues, including adipose tissues.[7] Aromatase is a crucial enzyme in the biosynthesis of estrogens, which are hormones that aid in the development of some forms of *Br Ca*.[8] The conversion of androgens into estrogens is catalyzed by aromatase.[9] Given the importance of estrogen production in encouraging the growth of *Br Ca*, aromatase has emerged as critical target for the search for anticancer agents in the treatment of *Br Ca*.[10] Aromatase inhibitors (AIs) are classified based on the difference between their chemical structures and mode of actions as steroidal and nonsteroidal AIs.[11] Among them, nonsteroidal AIs (NSAIs) have received increased interest in clinical applications due to their reversible inhibitory nature.[12] Among these, third generation NSAIs (*i.e.*; Letrozole, anastrozole and vorozole) were identified as the most effective treatments for estrogen-dependent post-menopausal women with advanced breast cancer.[12] However, their notable adverse effects (*i.e.*, decreased bone density and increased risk of cardiovascular diseases) and potential drug resistance in prolonged usage remain difficult challenges to

[a]*Department of Biotechnology, College of Sciences, Taif University, P.O. Box 11099, Taif 21944, Saudi Arabia*
[b]*Department of Pharmaceutics, College of Pharmacy, Al-Naji University, Baghdad 10015, Iraq*
[c]*Department of Chemistry, Science and Arts College, King Abdulaziz University, Rabigh, Saudi Arabia*
[d]*Regenerative Medicine Unit, King Fahd Medical Research Centre, King Abdulaziz University, Jeddah, Saudi Arabia*
[e]*Department of Chemistry, College of Science, Princess Nourah bint Abdulrahman University, P.O. Box 84428, Riyadh 11671, Saudi Arabia*
[f]*Chemistry Department, College of Science, Umm Al-Qura University, 21955, Makkah, Saudi Arabia*
[g]*Department of Chemistry, Faculty of Science, King Khalid University, Abha 61413, Saudi Arabia*
[h]*Chemistry Department, Faculty of Science, Port Said University, 42511 Port Said, Egypt. E-mail: amalyoussef840@gmail.com; a.moustafa@sci.psu.edu.eg*

resolve.[13] Accordingly, the development of novel NSAIs with improved potency and selectivity is still an active field of research in the modern medicinal chemistry.

Naphthalene nucleus is planar bicyclic molecule made up of two benzene rings that have fused together.[14] According to Huckel's rule, it is the simplest polycyclic aromatic hydrocarbon containing 10π electrons in its structure.[15] In medicinal chemistry, naphthalene scaffold constitute a versatile and adaptable platform.[16] It has been reported that the naphthalene scaffold is a good surrogate for the benzene ring, improving the active compounds' chemical and metabolic stability while maintaining pharmacology.[17] This scaffold's diverse biological activities resulting from structural modifications make it an attractive moiety in drug design advancement.[18] Derivatives based on naphthalene have been shown to exhibit a variety of antagonistic properties, including anticancer, antimicrobial, antiviral and antitubercular agents.[19–22] Naphthalene derivatives have been shown to exhibit anticancer properties through a variety of mechanistic pathways, like aromatase inhibitors, potent topoisomerase inhibitors and as microtubule polymerization inhibitors.[23–25] For example, Furomollugin **I** is a naturally occurring naphthalene-based compound revealed outstanding anticancer properties.[26] In addition, the naphthochalcone derivative Hymnpro **II** exhibited antiproliferative activity in several human solid tumor cell lines and suppressed xenograft tumor growth in nude mice.[27] Additionally, the antiproliferative effect of naphthalen-1-yl linked pyrazole derivative **III** on MCF-7 cells was associated with cellular cycle arrest followed by apoptosis.[28] Also, the bis-naphthalene-sulphonamide derivative **IV** was identified as aromatase inhibitors with IC_{50} value of 0.21 μM relative to reference standard Letrozole (IC_{50} = 0.19 μM) with high safety profile favouring cancer cells.[29]

In the recent years, acrylamide scaffold is appreciated owing to their therapeutic properties which have been reported for certain derivatives especially in the treatment of *Br Ca* cells.[30] The search on acrylamide-based covalent inhibitors has advanced significantly, showing promise in a number of therapeutic domains, especially as tubulin and kinase inhibitors for the management of different cancer types.[31,32] An acrylamide fragments are very beneficial for joining arms with variously substituted aryl fragments to create side chain components.[33] The structure of important moieties such as urea and hydrazone moieties was replaced with an acrylamide fragment that was comparable in length and structure to these important moieties, thereby ensuring the formation of crucial hydrogen bonding with the amino group in the target protein or receptor.[34,35] 2,3-Disubstituted acrylamide-bearing derivative **V** (Fig. 1) explored the highest potency against MCF-7 breast cancer cells through its inhibitory effect on EGFR-TK.[36]

Based on the above reported studies we understood the potential of naphthalene and acrylamide conjugates in the treatment of cancer. In this context, the synthesis of a new series of naphthalen-1-yloxyacetamide-tethered acrylamide conjugates was reported (Fig. 2). The target conjugates were created from the starting material, 1-naphthol following the general pathway reported in Scheme 1. All the created conjugates were confirmed by various methods of spectral analysis such as ^{1}H-NMR and ^{13}C-NMR. The newly synthesized compounds were evaluated for their cytotoxicity against MCF-7 *Br Ca* cell line to investigate their potential as chemotherapeutic agents. The most active naphthalen-1-yloxyacetamide-tethered acrylamide conjugate **5d** was subjected to cytofluorimetric analysis and aromatase inhibitory activity to explore the mechanism of cellular death. Moreover, the ability of compound **5d** to induce apoptosis/necrosis in MCF-7 *Br Ca* cells was determined. Furthermore, its impact on the protein expression levels of apoptotic markers was measured.

2. Results and discussion

2.1. Chemistry

The synthetic route of the designed naphthalen-1-yloxyacetamide tethered acrylamide conjugates **5a–j** and **6a**, **6b** were presented in Scheme 1. The target conjugates were prepared from the root starting material; naphthalen-1-yloxy acetic acid **2** which was achieved from the low-cost 1-naphthol and 2-bromoacetic acid *via* classical nucleophilic substitution reaction of phenolic OH group with alkyl bromide group.[37] Ethyl naphthalen-1-yloxy acetate **3** was synthesized *via* classical condensation reaction by refluxing the naphthalen-1-yloxy acetic acid **2** with pure ethanol in the presence of catalytic concentrated sulphuric acid.[38] Adopting condensation reaction of **3** with hydrazine hydrate in pure ethanol gave the key intermediate, naphthalen-1-yloxy acetic acid hydrazide **4**.[39] The formation of novel naphthalen-1-yloxyacetamide tethered 2,3-disubstituted acrylamide conjugates **5a–j** and **6a**, **6b** was accomplished *via* the reaction of equimolar amounts of naphthalen-1-yloxy acetic acid hydrazide **4** with respective ethyl 2,3-disubstituted acrylate ester in refluxing pure ethanol with a catalytic base of fused sodium acetate. The structures of new conjugates were confirmed by elemental analysis and spectral data. Both the analytical and spectral data (^{1}H-NMR and ^{13}C-NMR) of newly synthesized naphthalen-1-yloxyacetamide tethered acrylamide conjugates **5a–j** and **6a**, **6b** in DMSO-d_6 were completely in accordance with the expected structures as indicated in the SI. ^{1}H-NMR spectrum of naphthalen-1-yloxyacetamide tethered 2-(benzamido)-3-(4-methoxyphenyl) acrylamide **5d**, as example, demonstrated the presence of three singlets in the range at δ 10.33–9.89 ppm integrated one proton each corresponding to three amidic NH protons. The multiplet signals in the aromatic region at δ 8.44–6.97 were ascribed to 1-naphthyl, phenyl and olefinic protons. The ^{1}H-NMR spectrum also exhibited the characteristic signals for the methylene and methoxy protons. These proton signals were observed at δ 4.86 and 3.76 ppm, respectively. The ^{13}C-NMR spectrum of conjugate **5d** disclosed characteristic signals resonating around δ 160.19–106.21 ppm that were attributed to 1-naphthyl, phenyl and acrylate carbons. The three amide carbonyl (C=O) functionalities displayed in the ^{13}C-NMR spectrum at the δ 167.11–164.96 ppm. The presence of carbon peaks at 66.98 ppm confirms the linkage of methylene group with acrylamide moiety. In addition to a resonance peak at δ 55.68 ppm was attributed to the methoxy carbon confirming the proposed structure.

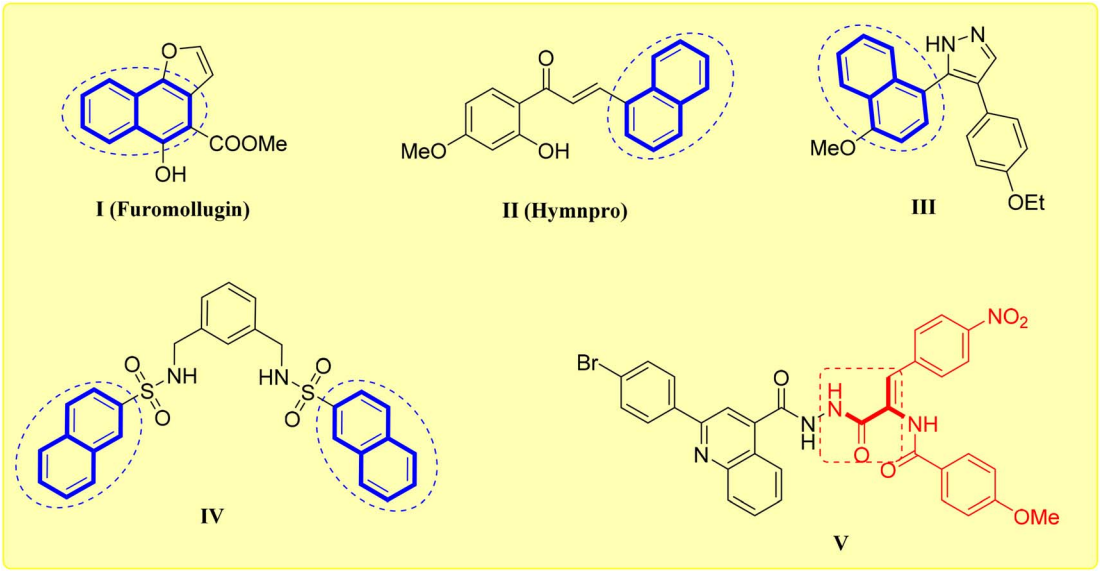

Fig. 1 Naphthalene I–IV and 2,3-disubstituted acrylamide V derivatives as anticancer agents.

2.2. Biological evaluation

2.2.1. Cytotoxic activity against MCF-7 *Br Ca* cells. To assess the antiproliferative effects of the target naphthalen-1-yloxyacetamide tethered acrylamide conjugates **5a–j** and **6a**, **6b**, a colorimetric MTT technique was utilized against MCF-7 *Br Ca* cell line.[40] The results were listed as an IC_{50} values with antitumor drugs Doxorubicin (Dox) and Tamoxifen (Tam) were included as reference drugs in this study. As demonstrated in Table 1, the majority of the investigated naphthalen-1-yloxyacetamide tethered acrylamide conjugates revealed good cytotoxicity with IC_{50} value ranging from 2.33–51.80 μM. In descending pattern, conjugates **5d**, **5e** and **5c** were the most active conjugates against MCF-7 cells with IC_{50} values of 2.33, 3.03 and 7.39 μM, respectively. Interestingly, conjugates **5d** and **5e** showed comparable cytotoxic action with that of Dox against MCF-7 cells (IC_{50} = 6.89 μM). The activity of conjugates **5d** and **5e** was 2.96- and 2.27-fold that of Dox, respectively. In addition, the cytotoxic activity value of conjugate **5c** (IC_{50} = 7.39 μM) was nearly equivalent to that of the standard Dox. Considering aryl group at C3 position of acrylamide moiety, conjugates **5a** and **5b** which include 4-chlorophenyl and 4-bromophenyl showed a significant drop in cytotoxic activity against MCF-7 *Br Ca* cell line, with IC_{50} value of 51.80 and 30.71 μM, respectively, in comparison to Dox (IC_{50} = 6.89 μM). In addition, the substituting 3-(4-bromophenyl)acrylamide for 3-(3,5-dibromo-4-hydroxyphenyl)acrylamide substituent in compound **5g** (IC_{50} = 18.46 μM) results in a rise of the biological activity. Additionally, activity increased with the incorporation of a 4-nitrophenyl moiety at C3 position of acrylamide moiety; **5c** (IC_{50} = 7.39 μM). On the other hand, the biological activity increased and became stronger with the aryl group having electron-releasing substituents at C3 position of acrylamide moiety in naphthalen-1-yloxyacetamide-3-(4-methoxyphenyl)acrylamide **5d** (IC_{50} = 2.33 μM) and naphthalen-1-yloxyacetamide-3-(4-dimethylaminophenyl)acrylamide **5e** (IC_{50} = 3.03 μM). Furthermore, the activity against MCF-7 *Br Ca* cells was lowered by **5h** (IC_{50} = 25.90 μM) with 2,3,4-trimethoxyphenyl or its positional isomer **5i** (IC_{50} = 16.94 μM) with 3,4,5-trimethoxyphenyl moiety. Again, conjugate **6a** (IC_{50} = 9.18 μM) having furan-2-yl moiety at C3 position of acrylamide series had one third of Dox's cytotoxic action. Alternatively, with respect to arylamide moiety attached to C2 position of acrylamide moiety, the presence of 4-methoxybenzamide group in conjugates **5j** (IC_{50} = 21.21 μM) and **6b** (IC_{50} = 11.52 μM) decreased the activity compared to their corresponding 2-(unsubstituted benzamide) acrylamide in conjugates **5i** (IC_{50} = 16.94 μM) and **6a** (IC_{50} = 9.18 μM).

2.2.2. Aromatase inhibition assay. Aromatase inhibitors are a potential path in searching for new therapies that can treat cancer, particularly hormone-dependent *Br Ca*.[41] It has been shown that *Br Ca* cells displayed an enhanced expression of aromatase, and, thus, produce higher concentrations of estrogens than normal cells.[42] Therefore, aromatase inhibitors are the first-line therapy for *Br Ca* management.[43] In this regard, to determine whether constructed naphthalen-1-yloxyacetamide-tethered acrylamide conjugates trigger aromatase enzyme inhibition in MCF-7 *Br Ca* cells to induce apoptotic cellular death. The most potent conjugates **5c**, **5d** and **5e** (at five different concentrations) were examined for their potency as aromatase inhibitors using ELISA method kit. Letrozole was utilized as reference standard in this study. Results presented in Fig. 3 clearly indicated the noteworthy decrease in the aromatase enzyme after treatment with investigated compounds **5c**, **5d** and **5e** with IC_{50} ranges of 0.078–0.143 μM, when compared to the reference Letrozole (aromatase IC_{50} = 0.068 μM). Compound **5d** the most potent antiproliferative agents, displayed the utmost inhibitory efficacy against aromatase with IC_{50} value of 0.078 μM, which was comparable to Letrozole (aromatase IC_{50} = 0.068 μM). The results also showed that,

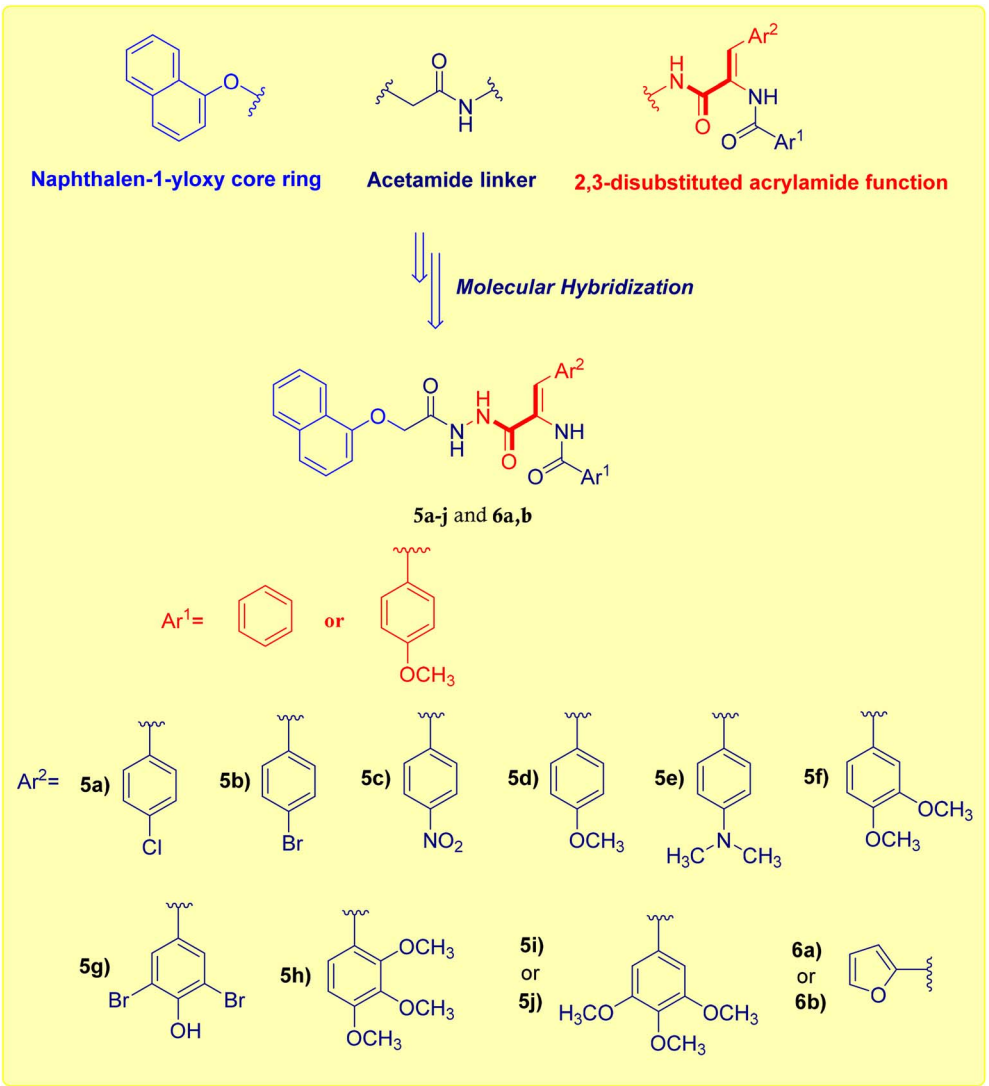

Fig. 2 Design pathway adopted for naphthalen-1-yloxyacetamide-tethered acrylamide conjugates 5a–j and 6a, 6b.

compared to Letrozole, the other investigated naphthalen-1-yloxytacetamide tethered acrylamides **5c** and **5e** showed good aromatase inhibition activity (IC_{50} values of 0.143 and 0.093 μM, respectively). The results of this assay method indicated that naphthalene-1-yloxtacetamide-acrylamides **5d** and **5e** had substantial antiproliferative activity against MCF-7 *Br Ca* cells and as aromatase inhibitors.

2.2.3. *In vitro* DNA flow cytometry for compound 5d on MCF-7 *Br Ca* cells. It is frequently utilized in cell biology to comprehend growth regulation, cell proliferation and the impact of both drugs and genetic alterations on cellular division.[44] Recognizing and manipulating the phase at which cell cycle arrest occurs can improve the therapeutic efficacy and selectivity of chemotherapeutic drugs, as many cancer therapies target rapidly proliferating cells.[45] The most cytotoxic naphthalen-1-yloxyacetamide-tethered acrylamide conjugate, **5d**, was chosen in order to further assess its impact on the advancement on cell cycle in MCF-7 *Br Ca* cells. In this context, MCF-7 *Br Ca* cells were hatched with the examined conjugate, **5d**, at the IC_{50} value for 48 h, and then the DNA content was measured by flow cytometry utilizing FACS Calibur device. There was also a control experiment that receives no treatment. According to Flow cytometric study, naphthalen-1-yloxyacetamide-tethered acrylamide conjugate **5d** treatment causes a G1 stoppage that is almost 1.4-times greater than that of the control (Fig. 4). The accumulation of cells in G1 phase suggest that conjugate **5d** may play a part in inhibiting cellular proliferation and causing cell death. These findings showed that the analyzed naphthalen-1-yloxyacetamide-tethered acrylamide conjugate **5d** inhibited cell proliferation at the G1 phase of the cellular cycle.

2.2.4. *In vitro* apoptosis identification by FITC-Annexin V staining. Tissue homeostasis, immunological response, and appropriate development all depend on apoptosis.[46] Chromosomal DNA fragmentation into tiny units known as oligomers, apoptotic body formation and nuclei condensation and fragmentation are all signs of apoptotic cell death.[47] The abnormal suppression of apoptosis is a hallmark of cancer and

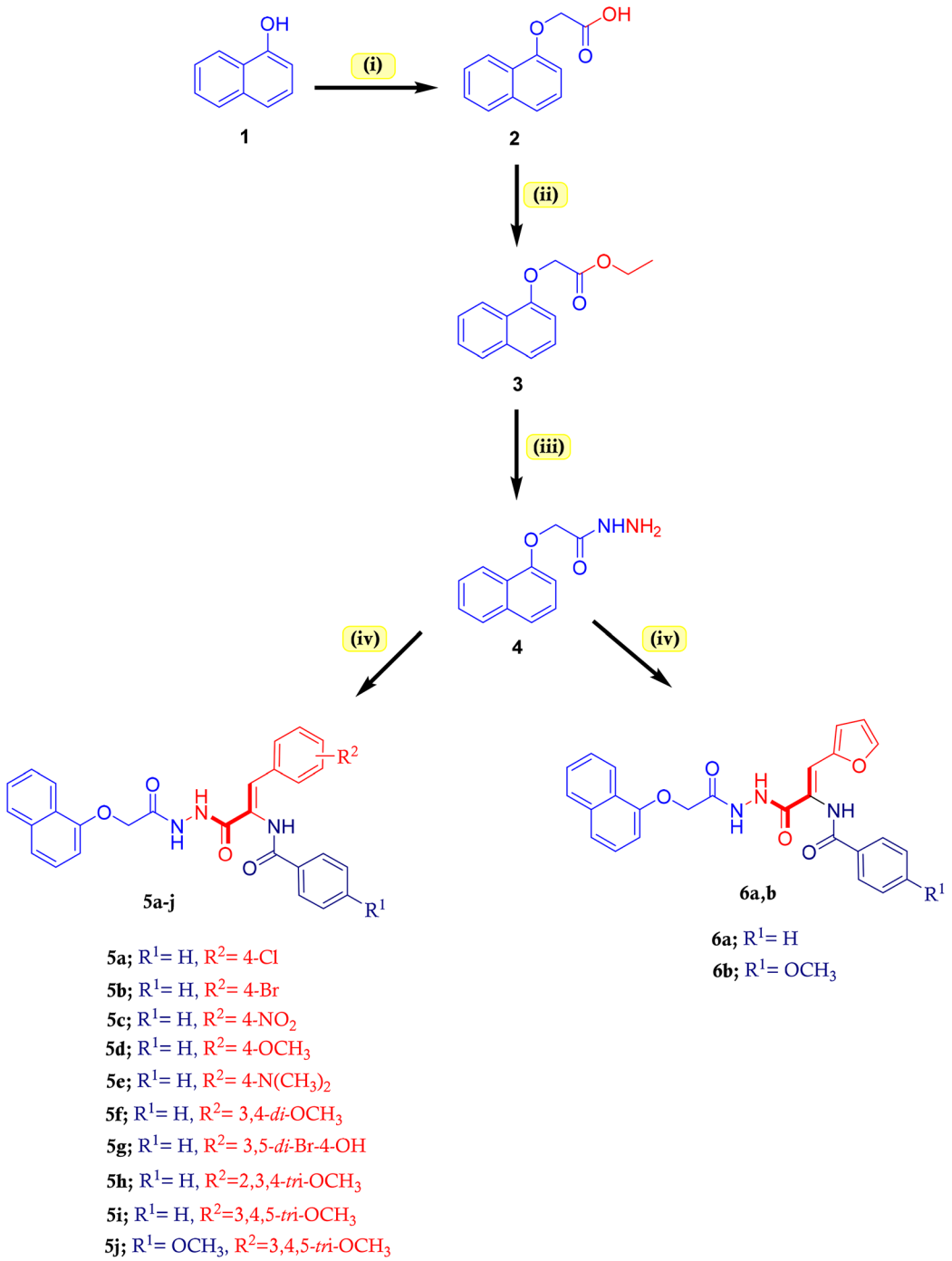

Scheme 1 Synthesis of naphthalen-1-yloxyacetamide-tethered 2,3-disubstituted acrylamide conjugates **5a–j** and **6a**, **6b**. Condition: (i) $BrCH_2COOH$, K_2CO_3, acetone, reflux 12 h; (ii) pure EtOH, AcOH, reflux 16 h; (iii) $NH_2NH_2{\cdot}H_2O$, EtOH, reflux 8 h; (iv) respective ethyl 2,3-disubstituted acrylate ester, NaOAc, EtOH, reflux 12–14 h.

autoimmune disease.[48] One key strategy for cancer prevention or treatment has been to induce apoptosis either directly, or after final differentiation, or after stopping the cell cycle.[49] To further evaluate the tumor suppression ability of naphthalen-1-yloxyacetamide tethered acrylamide conjugate **5d**, and to verify that the found G1 cells accumulation was caused by apoptosis, *Br Ca* cells treated with **5d** for 48 h was analyzed with Propidium Iodide (PI) and fluorochrome Annexin V stain for apoptosis determination. MCF-7 *Br Ca* cells treated with naphthalen-1-yloxyacetamide tethered acrylamide conjugate **5d** revealed an increased activity of both early apoptosis and late apoptosis sections (Fig. 5). Interestingly, the late apoptotic cells percentage showed a notable rise after treatment with compound **5d** from 0.14% in control untreated to 5.88% (42.0-fold increase). In addition, early apoptosis significantly boosted from 0.57% in the no treatment control to 19.17% (33.6-fold

Table 1 The cytotoxicity screening results of investigated naphthalen-1-yloxyacetamide tethered 2,3,-disubstituted acrylamide conjugates **5a–j** and **6a**, **6b**. Values represent the mean value ± SD ($n = 3$)

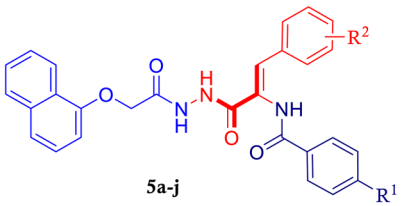

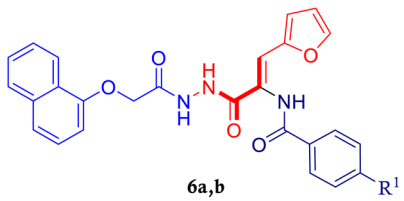

Compd no.	R^1	R^2	IC_{50} (μM) MCF-7
5a	–H	4-Cl	51.80 ± 1.51
5b	–H	4-Br	30.71 ± 1.18
5c	–H	4-NO_2	7.39 ± 0.86
5d	–H	4-OCH_3	2.33 ± 0.10
5e	–H	4-$N(CH_3)_2$	3.03 ± 0.48
5f	–H	3,4-Di-OCH_3	28.66 ± 1.45
5g	–H	3,5-Di-Br-4-OH	18.46 ± 1.26
5h	–H	2,3,4-Tri-OCH_3	25.90 ± 1.41
5i	–H	3,4,5-Tri-OCH_3	16.94 ± 0.82
5j	–OCH_3	3,4,5-Tri-OCH_3	21.21 ± 0.92
6a	–H	—	9.18 ± 0.66
6b	–OCH_3	—	11.52 ± 0.76
Dox	—	—	6.89 ± 0.13
Tam	—	—	10.49 ± 0.23

increase) upon treatment with conjugate **5d**. The experiment's outcome was consistent with the previous one, confirming that naphthalen-1-yloxyacetamide-tethered acrylamide conjugate **5d** demonstrated its cytotoxic impact *via* apoptosis-promoting activity.

2.2.5. *In vitro* Bax and Bcl2 levels assay. Programmed cell death, or apoptosis, is a complex series of biochemical processes.[50] Pro-apoptotic proteins include Bad, Bax, Bid and Bim, while anti-apoptotic members include Bcl-2 and Bc-LXI.[51,52] The anti-apoptotic proteins prevent cytochrome-c from

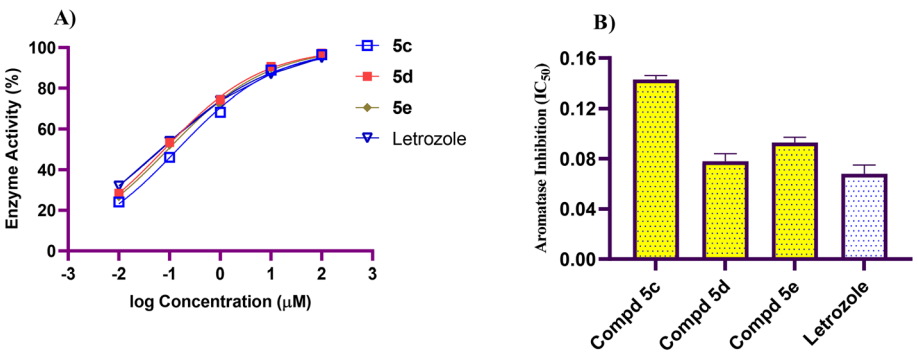

Fig. 3 (A) The impact of naphthalen-1-yloxtacetamide-tethered acrylamides **5c**, **5d**, **5e** and Letrozole at five different concentrations for IC_{50} determination of aromatase enzyme. (B) Graphical illustration of the IC_{50} values against aromatase enzyme in MCF-7 *Br Ca* cells treated with naphthalen-1-yloxtacetamide-tethered acrylamides **5c**, **5d**, and **5e** compared with Letrozole.

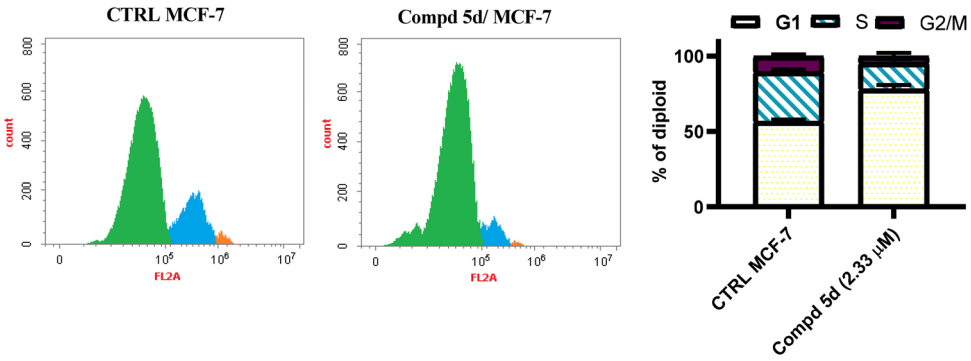

Fig. 4 Cell cycle disruption after naphthalene-1-yloxyacetamide tethered 2-(benzamide)-3-(4-methoxypheny)acrylamide conjugate **5d** treatment at indicated concentration analysis of MCF-7 *Br Ca* cell line.

release, which inhibits apoptosis, while pro-apoptotic members activate the release of cytochrome-*c*.[53] When there is a higher ratio of pro-apoptotic proteins than anti-apoptotic ones, the outer mitochondrial membrane becomes permeable leading to a cascade of events.[54] The cytochrome-*c* is released, which activates caspase 9, which in turn triggers caspase 3, which triggers apoptotic processes.[55] In this context, the most active naphthalen-1-yloxyacetamide tethered acrylamide conjugate **5d** was further studied for its impact on Bax and Bcl2 levels against MCF-7 *Br Ca* cell line using qRT-PCR technique. According to the data, the tested compound's Bax gen level increased noticeably compared with control. Compound **5d** which was bearing 3-(4-methoxyphenyl)acrylamide moiety possessed an overexpression of Bax level with 4.0-fold higher than untreated MCF-7 *Br Ca* cells. However, in contrast to negative control group, conjugate **5d** diminished the amount of Bcl-2 gene level in MCF-7 *Br Ca* cells by a factor of 0.3 (Fig. 6).

2.2.6. Apoptotic markers activation. An essential initiator caspase in the intrinsic apoptotic process is caspase 9.[56] It is essential for inducing cell death in response to internal stress such as oxidative stress, DNA damage, or oncogene activation conditions, which are frequently present in cancer cells.[57] Therefore, therapeutic strategies that enhance or restore its activity can potentially overcome apoptosis resistance in tumors.[58] In this context, naphthalene-1-yloxyacetamide tethered acrylamide conjugate **5d** were evaluated as caspase 9 activator against MCF-7 cells using qRT-PCR technique. The results are presented in Fig. 7. The results demonstrated that conjugate **5d** which was bearing 3-(4-methoxyphenyl)acrylamide moiety attached naphthalene-1-yloxyacetamide function boosted caspase 9 gene level compared to the controls. It is worth mentioning that, the level of caspase 9 protein level is increased 8.2-fold more than the negative control. The aforementioned findings could be interpreted as evidence that the apoptosis may be attributed to the up-regulation of caspase 9 which induced by the tested naphthalen-1-yloxyacetamide tethered acrylamide conjugate **5d**.

2.2.7. *In silico* ADME prediction. Using the Swiss ADME online tool created by the Swiss institute of bioinformatics (SIB), computer-assisted ADME profile and drug-like characteristic of the most potent conjugates **5c**, **5d** and **5e** was carried out to evaluate the pharmacokinetic features. Letrozole was utilized as

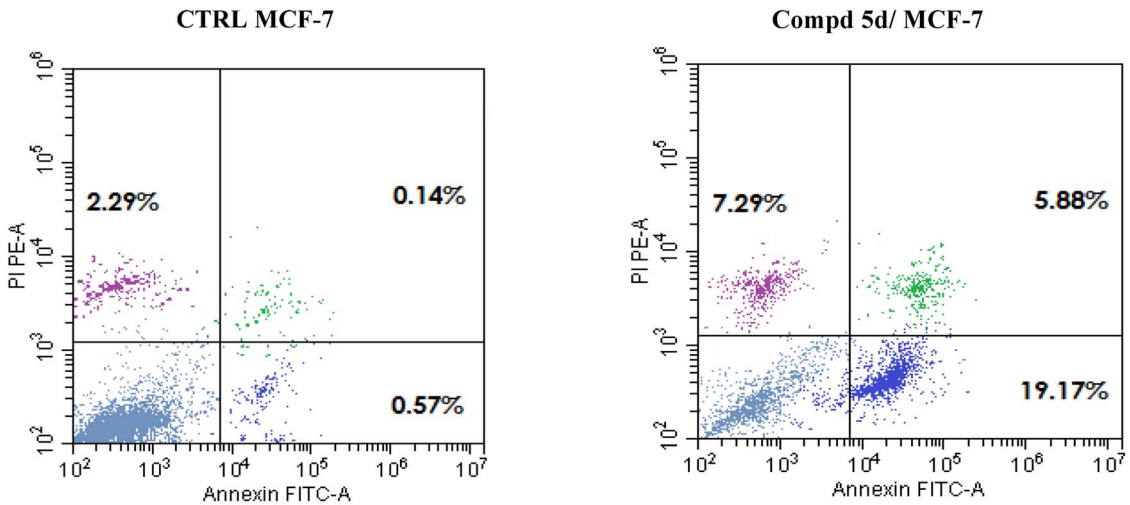

Fig. 5 Cytofluorimetric analysis of MCF-7 *Br Ca* cell line treated with naphthalene-1-yloxyacetamide tethered 2-(benzamide)-3-(4-methoxypheny)acrylamide conjugate **5d** at the IC_{50} concentration and compared to the negative controls.

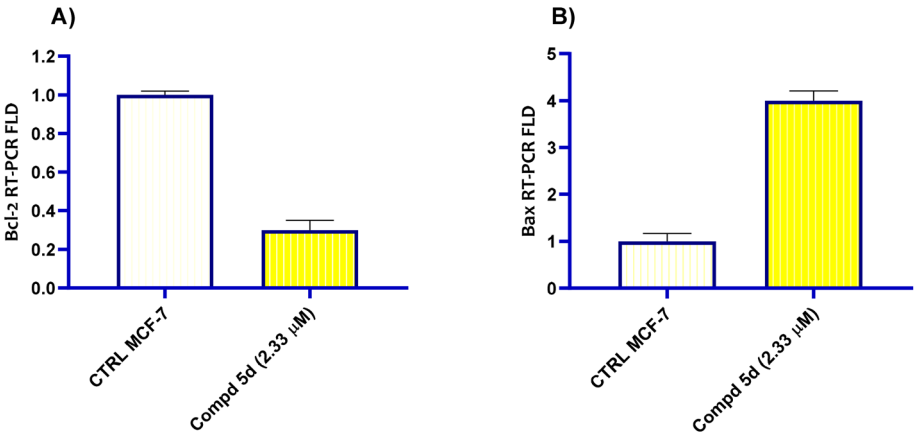

Fig. 6 Bar graph of naphthalene-1-yloxyacetamide tethered 2-(benzamide)-3-(4-methoxypheny)acrylamide conjugate **5d** treatment at indicated concentration analysis of Bcl-2 and Bax levels in MCF-7 *Br Ca* cell line. (A) Effect on Bcl2; (B) effect on Bax.

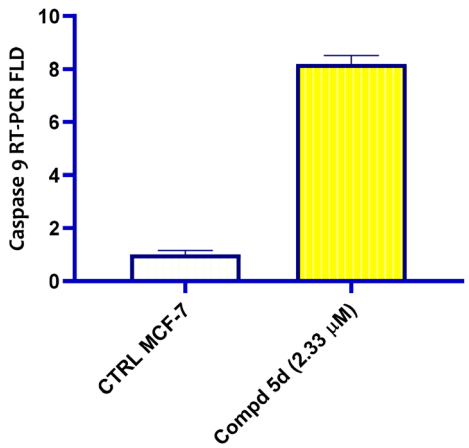

Fig. 7 Bar graph of naphthalen-1-yloxyacetamide tethered 2-(benzamide)-3-(4-methoxypheny)acrylamide conjugate **5d** treatment at indicated concentration analysis of caspase 9 level in MCF-7 *Br Ca* cell line using qRT-PCR technique.

reference molecule. It was anticipated that naphthalen-1-yloxyacetamide-tethered acrylamides **5d** and **5e** to have high GIT absorption as it was positioned in the white region of human intestinal absorption (HIA) in boiled egg chart (Fig. 7). In addition, conjugates **5d** and **5e** demonstrated good predicted absorption levels, while compound **5c** displayed poor range. Furthermore, the investigated conjugates **5c**, **5d** and **5e** may not have the capacity to penetrate the BBB as it was located outside the yellow region which denotes the BBB penetration, and therefore, it might be used wisely for peripheral tumors with no CNS problems. Moreover, the red circle in Fig. 8 denoted that the investigated naphthalen-1-yloxyacetamide-tethered acrylamides **5c**, **5d** and **5e** was not a substrate for P-glycoprotein (PGP), so it can't be pumped by it out of the cells into the gut lumen, into the bile, or into the urine. This prediction suggested that all the investigated conjugates may be expected to enhance intracellular drug accumulation and boost therapeutic efficacy. In conclusion, it was found that naphthalen-1-yloxyacetamide-tethered acrylamides **5d** and **5e** exhibited not only significant biological activity, but also an acceptable predicted ADME and physicochemical aspects.

3. Conclusions

In summary, a new set of naphthalen-1-yloxyacetamides **5a–j** and **6a**, **6b** having a 2,3-disubstituted acrylamide moiety has been successfully synthesized by a facile method. These chemical conjugates were characterized by elemental analysis as well as ^{1}H-NMR, ^{13}C-NMR spectroscopic tools. In addition, these conjugates were evaluated for their antiproliferative activity against the MCF-7 *Br Ca* cell line using the MTT colorimetric technique. Among all the examined conjugates, **5c**, **5d**, and **5e** demonstrated notable cytotoxic activity with IC_{50} values of 2.33, 3.03, and 7.39 μM, respectively, compared to the standard Dox (IC_{50} = 6.89 μM). The *in vitro* enzyme inhibitory assay of **5c**, **5d**, and **5e** against aromatase inhibition was evaluated, and the obtained results were promising (IC_{50} values = 0.143, 0.078 and 0.093 μM, respectively) compared with Letrozole (IC_{50} = 0.068 μM) as standard aromatase inhibitory drug. Further, a representative promising conjugate in cytotoxic and aromatase inhibition assays was subjected to further mechanistic evaluation studies; cell cycle analysis was carried out on MCF-7 *Br Ca* cell line, which elicited G1 phase arrest. The mechanistic studies also demonstrated that naphthalen-1-yloxyacetamide **5d** bearing a 2-benzamido-3-(4-methoxyphenyl)acrylamide moiety provoked apoptosis in MCF-7 *Br Ca* cells *via* the expressive downregulation of the anti-apoptotic protein Bcl-2, as well as increasing Bax and caspase 9 levels with regard to untreated controls. In conclusion, we identified **5d**, which was bearing a 3-(4-methoxyphenyl)acrylamide moiety connected to naphthalen-1-yloxyacetamide function as a cytotoxic agent which inhibited aromatase enzyme and stopped the cell cycle at the point of G1. Hence, we may conclude that naphthalen-1-yloxyacetamide **5d**, which contains a 2-benzamido-3-(4-methoxyphenyl)acrylamide moiety, was emerged as potential candidate for future *in vivo* investigation for pharmacokinetics and toxicity properties.

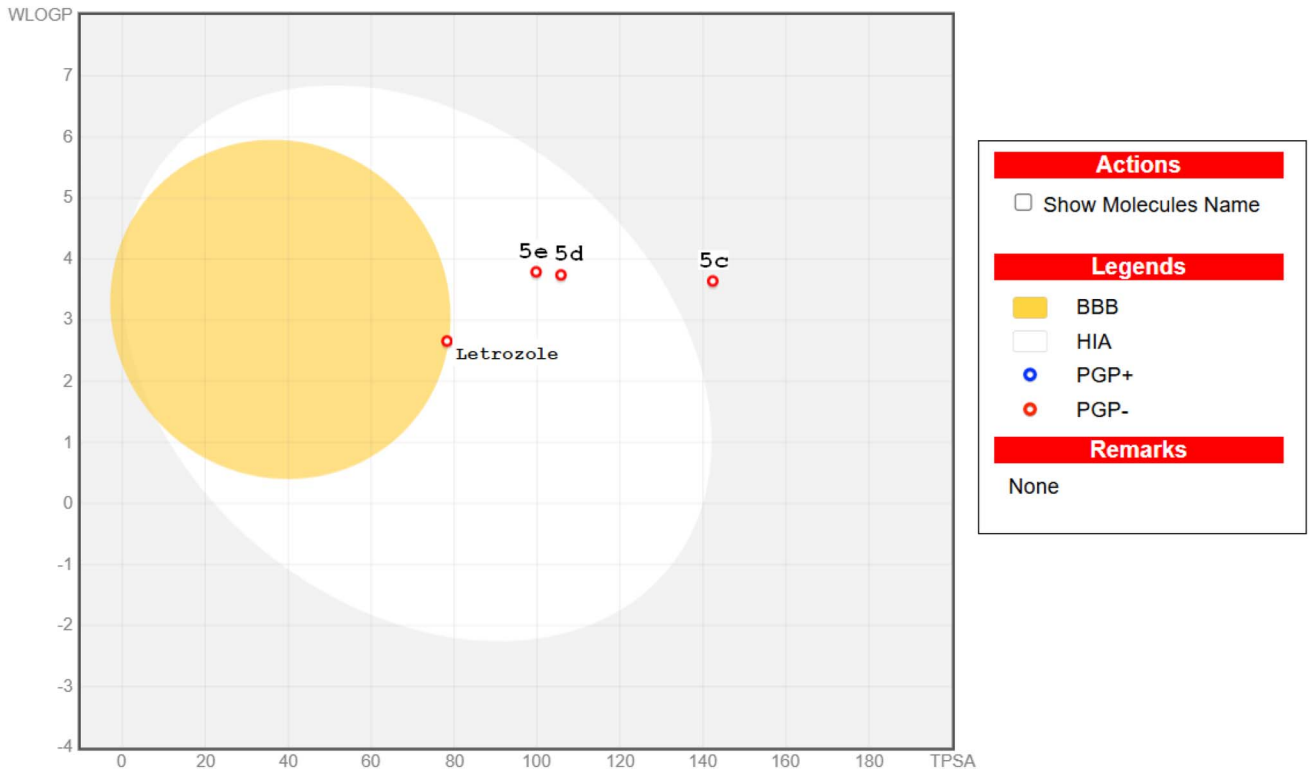

Fig. 8 *In silico* ADME predictive plot of the synthesized naphthalen-1-yloxyacetamide-tethered acrylamides **5c**, **5d**, **5e** and Letrozole from Swiss ADME online tool.

4. Experimental

4.1. Chemistry

4.1.1. General reaction procedure for the synthesis of (*Z*)-*N*-(1-aryl-3-(2-(2-(naphthalen-1-yloxy)acetyl)hydrazineyl)-3-oxoprop-1-en-2-yl)arylamides 5a–j and 6a, 6b. To a suspension of naphthalen-1-yloxyacetohydrazide **3** (1.08 g, 5 mmol), respective ethyl 2-benzamido-3-(4-chlorophenyl)acrylate (1.65 g, 5 mmol) in pure ethanol (20 mL) was added catalytic amount of fused sodium acetate. The reaction mixture was refluxed until complete conversion as monitored by TLC (around 12–14 h). After cooled, the precipitates obtained were filtered, washed and crystallized with ethanol/H_2O (3 : 1) to attain pure (*Z*)-*N*-(1-(4-chlorophenyl)-3-(2-(2-(naphthalen-1-yloxy)acetyl) hydrazineyl)-3-oxoprop-1-en-2-yl)benzamide (**5a**) as yellow solids. All the other naphthalene-1-yloxyacetamide-tethered acrylamide conjugates **5b–j** and **6a**, **6b** were obtained in a similar reaction procedure of **5a** in moderate to good yields.

*4.1.1.1. (Z)-N-(1-(4-Chlorophenyl)-3-(2-(2-(naphthalen-1-yloxy)acetyl)hydrazineyl)-3-oxoprop-1-en-2-yl)benzamide (**5a**).* Yellow solid, yield 77%; mp: 239–241 °C. ^{1}H-NMR (400 MHz, DMSO-d_6) δ 10.38 (s, 2H, 2NH), 10.01 (s, 1H, NH), 8.38 (dd, J = 15.9, 7.6 Hz, 1H), 8.01 (d, J = 7.4 Hz, 1H), 7.89 (d, J = 7.2 Hz, 2H), 7.61 (d, J = 8.0 Hz, 2H), 7.59–7.48 (m, 6H), 7.44 (t, J = 7.3 Hz, 3H), 7.28 (s, 1H, $H_{C=C}$), 7.00 (d, J = 6.8 Hz, 1H), 4.85 (d, J = 9.8 Hz, 2H, O**C**H_2N). MS (*m*/*z*, %): 499.48 (M^+, 19.09), 186.08 (100). Analysis: calc. for $C_{28}H_{22}ClN_3O_4$ (499.95): C 67.27, H 4.44, N 8.41%, found: C 67.41, H 4.52, N 8.32%.

*4.1.1.2. (Z)-N-(1-(4-Bromophenyl)-3-(2-(2-(naphthalen-1-yloxy)acetyl)hydrazineyl)-3-oxoprop-1-en-2-yl)benzamide (**5b**).* Orange solid, yield 82%; mp: 222–224 °C. ^{1}H-NMR (400 MHz, DMSO-d_6) δ 10.35 (s, 2H, 2NH), 10.02 (s, 1H, NH), 8.39–8.33 (m, 1H), 8.02–7.99 (m, 1H), 7.93–7.84 (m, 2H), 7.63–7.59 (m, 2H), 7.57 (s, 2H), 7.54 (d, J = 2.9 Hz, 3H), 7.53–7.51 (m, 2H), 7.42 (td, J = 7.9, 3.9 Hz, 2H), 7.25 (s, 1H, $H_{C=C}$), 6.99 (dd, J = 7.7, 4.6 Hz, 1H), 4.85 (d, J = 8.5 Hz, 2H, O**C**H_2N). ^{13}C-NMR (101 MHz, DMSO-d_6) δ: 167.06, 166.35, 164.68, 153.82, 134.49, 133.98, 133.80, 132.23, 131.99, 131.75, 129.94, 129.19, 128.76, 128.42, 127.83, 127.01, 126.47, 125.77, 125.29, 122.59, 122.51, 121.16, 106.15, 66.85. MS (*m*/*z*, %): 544.94 (M^+, 20.69), 441.08 (100). Analysis: calc. for $C_{28}H_{22}BrN_3O_4$ (544.41): C 61.78, H 4.07, N 7.72%, found: C 61.65, H 3.96, N 7.86%.

*4.1.1.3. (Z)-N-(3-(2-(2-(Naphthalen-1-yloxy)acetyl)hydrazineyl)-1-(4-nitrophenyl)-3-oxoprop-1-en-2-yl)benzamide (**5c**).* Pale yellow solid, yield 85%; mp: 247–249 °C. ^{1}H-NMR (400 MHz, DMSO-d_6) δ 10.44 (s, 2H, 2NH), 10.19 (s, 1H, NH), 8.38–8.33 (m, 1H), 8.25–8.21 (m, 2H), 8.02–7.97 (m, 2H), 7.91–7.88 (m, 1H), 7.83 (d, J = 8.8 Hz, 2H), 7.61 (t, J = 7.4 Hz, 1H), 7.57–7.54 (m, 3H), 7.52 (d, J = 4.3 Hz, 2H), 7.42 (t, J = 8.1 Hz, 1H), 7.30 (s, 1H, $H_{C=C}$), 7.02–6.96 (m, 1H), 4.85 (s, 2H, O**C**H_2N). ^{13}C-NMR (101 MHz, DMSO-d_6) δ: 167.14, 166.42, 164.45, 153.82, 147.17, 141.56, 134.50, 133.79, 132.53, 132.38, 130.73, 128.80, 128.48, 127.84, 127.27, 127.03, 126.48, 125.78, 125.30, 124.12, 122.50, 121.17, 106.15, 66.83. MS (*m*/*z*, %): 510.91 (M^+, 38.18), 80.00 (100). Analysis: calc. for $C_{28}H_{22}N_4O_6$ (510.51): C 65.88, H 4.34, N 10.97%, found: C 66.02, H 4.48, N 10.84%.

*4.1.1.4. (Z)-N-(1-(4-methoxyphenyl)-3-(2-(2-(naphthalen-1-yloxy)acetyl)hydrazineyl)-3-oxoprop-1-en-2-yl)benzamide (**5d**).* Orange solid, yield 79%; mp: 224–226 °C. ^{1}H-NMR (400 MHz, DMSO-d_6) δ 10.33 (s, 1H, NH), 10.14 (s, 1H, NH), 9.89 (s, 1H, NH), 8.44–8.37 (m, 1H), 8.03 (d, J = 7.3 Hz, 2H), 7.90 (dd, J = 6.7, 2.6 Hz, 2H), 7.59–7.56 (m, 2H), 7.55–7.51 (m, 4H), 7.43 (t, J = 8.0 Hz, 2H), 7.32 (s, 1H, $H_{C=C}$), 6.97 (dd, J = 21.6, 8.0 Hz, 3H), 4.86 (s, 2H, O**CH**$_2$N), 3.76 (s, 3H, OCH_3). ^{13}C-NMR (101 MHz, DMSO-d_6) δ: 167.11, 166.27, 164.96, 160.19, 153.73, 134.51, 132.02, 131.69, 130.85, 128.70, 128.41, 128.38, 127.83, 127.07, 127.04, 126.47, 125.78, 125.29, 125.27, 122.60, 121.26, 114.51, 106.21, 66.98, 55.68. MS (*m*/*z*, %): 495.40 (M^+, 18.67), 69.11 (100). Analysis: calc. for $C_{29}H_{25}N_3O_5$ (495.54): C 70.29, H 5.09, N 8.48%, found: C 70.17, H 5.21, N 8.63%.

*4.1.1.5. (Z)-N-(1-(4-(Dimethylamino)phenyl)-3-(2-(2-(naphthalen-1-yloxy)acetyl)hydrazineyl)-3-oxoprop-1-en-2-yl) benzamide (**5e**).* Red solid, yield 80%; mp: 228–230 °C. ^{1}H-NMR (400 MHz, DMSO-d_6) δ: 11.36 (s, 1H, NH), 10.32 (s, 1H, NH), 8.23 (d, J = 8.7 Hz, 1H), 7.93 (dt, J = 7.1, 1.4 Hz, 2H), 7.89–7.85 (m, 2H), 7.78 (dd, J = 18.3, 8.2 Hz, 2H), 7.52–7.48 (m, 2H), 7.44–7.38 (m, 3H), 7.34–7.28 (m, 2H), 7.20 (s, 1H, $H_{C=C}$), 6.83 (d, J = 8.9 Hz, 2H), 4.91 (d, J = 7.8 Hz, 2H, O**CH**$_2$N), 3.06 (s, 6H, N(**CH**$_3$)$_2$). ^{13}C-NMR (101 MHz, DMSO-d_6) δ: 168.02, 167.92, 167.25, 156.43, 155.75, 152.41, 135.32, 134.42, 131.76, 130.92, 129.80, 129.14, 128.24, 128.00, 127.34, 127.25, 126.95, 124.38, 121.73, 119.04, 112.30, 108.04, 107.82, 66.61, 40.07. MS (*m*/*z*, %): 508.92 (M^+, 10.34), 105.11 (100). Analysis: calc. for $C_{30}H_{28}N_4O_4$ (508.58): C 70.85, H 5.55, N 11.02%, found: C 70.97, H 5.39, N 10.88%.

*4.1.1.6. (Z)-N-(1-(3,4-Dimethoxyphenyl)-3-(2-(2-(naphthalen-1-yloxy)acetyl)hydrazineyl)-3-oxoprop-1-en-2-yl)benzamide (**5f**).* Orange solid, yield 74%; mp: 217–219 °C. ^{1}H-NMR (400 MHz, DMSO-d_6) δ: 10.74 (s, 1H, NH, NH), 10.38 (s, 1H, NH, NH), 9.86 (s, 1H, NH, NH), 8.44 (dd, J = 8.5, 1.4 Hz, 1H), 8.29–8.24 (m, 2H), 8.17–8.14 (m, 1H), 8.06 (dd, J = 8.8, 1.5 Hz, 2H), 7.86 (ddd, J = 8.4, 6.8, 1.4 Hz, 1H), 7.79 (d, J = 8.6 Hz, 1H), 7.75–7.67 (m, 1H), 7.62 (d, J = 8.9 Hz, 1H), 7.40 (s, 1H), 7.24 (s, 1H, $H_{C=C}$), 7.17 (d, J = 8.9 Hz, 1H), 7.09 (t, J = 9.0 Hz, 2H), 6.96 (d, J = 8.9 Hz, 1H), 3.88 (s, 2H, OCH_2, O**CH**$_2$N), 3.85 (s, 3H, OCH_3), 3.77 (s, 3H, OCH_3). ^{13}C-NMR (101 MHz, DMSO-d_6) δ: 166.15, 165.95, 165.41, 163.88, 162.46, 162.11, 160.29, 155.00, 148.30, 142.11, 137.77, 134.75, 132.45, 131.81, 131.04, 130.41, 129.73, 127.95, 126.96, 124.22, 117.13, 115.37, 115.11, 114.57, 113.98, 56.17, 55.92, 55.71. MS (*m*/*z*, %): 525.05 (M^+, 29.49), 225.40 (100). Analysis: calc. for $C_{30}H_{27}N_3O_6$ (525.56): C 68.56, H 5.18, N 8.00%, found: C 68.66, H 5.03, N 7.83%.

*4.1.1.7. (Z)-N-(1-(3,5-Dibromo-4-hydroxyphenyl)-3-(2-(2-(naphthalen-1-yloxy)acetyl)hydrazineyl)-3-oxoprop-1-en-2-yl) benzamide (**5g**).* Yellow solid, yield 73%; mp: 233–235 °C. ^{1}H-NMR (400 MHz, DMSO-d_6) δ 10.58 (s, 1H, NH), 10.40 (s, 1H, OH), 10.35 (s, 1H, NH), 10.11 (s, 1H, NH), 8.38 (dd, J = 15.8, 7.9 Hz, 1H), 7.99 (dd, J = 14.0, 5.8 Hz, 3H), 7.94–7.86 (m, 2H), 7.82 (s, 1H), 7.59 (d, J = 12.6 Hz, 2H), 7.53 (d, J = 7.9 Hz, 3H), 7.45–7.40 (m, 1H), 7.27 (d, J = 13.1 Hz, 1H, $H_{C=C}$), 6.99 (dd, J = 7.7, 5.1 Hz, 1H), 4.89–4.84 (m, 2H, O**CH**$_2$N). ^{13}C-NMR (101 MHz, DMSO-d_6) δ: 167.66, 167.13, 167.04, 153.82, 153.73, 135.63, 134.50, 133.95, 133.73, 133.38, 131.46, 128.78, 128.32, 127.83, 127.02, 126.47, 125.78, 125.30, 122.52, 121.17, 117.59, 112.18, 106.14, 66.87. MS (*m*/*z*, %): 639.65 (M^+, 10.70), 92.29 (100). Analysis: calc. for $C_{28}H_{21}Br_2N_3O_5$ (639.30): C 52.61, H 3.31, N 6.57%, found: C 52.50, H 3.43, N 6.71%.

*4.1.1.8. (Z)-N-(3-(2-(2-(Naphthalen-1-yloxy)acetyl) hydrazineyl)-3-oxo-1-(2,3,4-trimethoxyphenyl)prop-1-en-2-yl) benzamide (**5h**).* Orange solid, yield 75%; mp: 211–213 °C. ^{1}H-NMR (400 MHz, DMSO-d_6) δ 10.27 (s, 2H, 2NH), 9.86 (s, 1H, NH), 8.40–8.35 (m, 1H), 8.00 (d, J = 7.7 Hz, 2H), 7.89 (dd, J = 6.7, 3.0 Hz, 1H), 7.56–7.52 (m, 5H), 7.43 (d, J = 3.0 Hz, 2H), 7.39–7.34 (m, 1H, $H_{C=C}$), 7.00 (dd, J = 8.0, 3.2 Hz, 2H), 6.84–6.74 (m, 1H), 4.85 (d, J = 11.2 Hz, 2H, O**CH**$_2$N), 3.85 (s, 3H, OCH_3), 3.78 (s, 3H, OCH_3), 3.76 (s, 3H, OCH_3). ^{13}C-NMR (101 MHz, DMSO-d_6) δ: 167.10, 166.30, 164.89, 154.62, 153.83, 152.73, 150.13, 149.29, 142.06, 134.50, 132.06, 130.05, 128.68, 128.42, 127.88, 127.01, 126.51, 125.76, 125.29, 124.15, 122.60, 121.27, 121.14, 108.44, 106.21, 66.97, 61.88, 60.90, 56.38. MS (*m*/*z*, %): 555.93 (M^+, 41.18), 85.64 (100). Analysis: calc. for $C_{31}H_{29}N_3O_7$ (555.59): C 67.02, H 5.26, N 7.56%, found: C 66.86, H 5.38, N 7.69%.

*4.1.1.9. (Z)-N-(3-(2-(2-(Naphthalen-1-yloxy)acetyl) hydrazineyl)-3-oxo-1-(3,4,5-trimethoxyphenyl)prop-1-en-2-yl) benzamide (**5i**).* Orange solid, yield 81%; mp: 216–218 °C. ^{1}H-NMR (400 MHz, DMSO-d_6) δ: 10.41 (s, 1H, NH), 10.26 (s, 1H, NH), 10.00 (s, 1H, NH), 8.42–8.33 (m, 1H), 8.08 (d, J = 7.7 Hz, 2H), 7.91–7.87 (m, 1H), 7.64–7.56 (m, 2H), 7.53 (d, J = 7.0 Hz, 4H), 7.42 (t, J = 8.0 Hz, 1H), 7.38 (s, 1H, $H_{C=C}$), 7.02 (d, J = 6.6 Hz, 1H), 6.98 (s, 2H), 4.84 (s, 2H), 3.66 (s, 3H, OCH_3), 3.61 (s, 6H, 2OCH_3). ^{13}C-NMR (101 MHz, DMSO-d_6) δ: 166.84, 166.32, 164.52, 153.87, 153.04, 138.59, 134.50, 134.07, 132.20, 131.42, 129.80, 128.82, 128.67, 128.36, 127.83, 127.00, 126.48, 125.75, 125.31, 122.52, 121.11, 107.62, 106.16, 66.98, 60.51, 56.04. MS (*m*/*z*, %): 585.32 (M^+, 33.92), 137.89 (100). Analysis: calc. for $C_{31}H_{29}N_3O_7$ (555.59): C 67.02, H 5.26, N 7.56%, found: C 67.14, H 5.33, N 7.46%.

*4.1.1.10. (Z)-4-Methoxy-N-(3-(2-(2-(naphthalen-1-yloxy)acetyl) hydrazineyl)-3-oxo-1-(3,4,5-trimethoxyphenyl)prop-1-en-2-yl) benzamide (**5j**).* Orange solid, yield 76%; mp: 225–227 °C. ^{1}H-NMR (400 MHz, DMSO-d_6) δ: 10.32 (s, 1H, NH), 10.08 (s, 1H, NH), 9.82 (s, 1H, NH), 8.36 (d, J = 7.8 Hz, 1H), 8.05 (d, J = 8.6 Hz, 2H), 7.91–7.87 (m, 1H), 7.59–7.53 (m, 2H), 7.52 (s, 1H), 7.42 (t, J = 7.9 Hz, 1H), 7.33 (s, 1H, $H_{C=C}$), 7.05 (d, J = 8.7 Hz, 2H), 7.01 (d, J = 7.0 Hz, 1H), 6.97 (s, 2H), 4.83 (s, 2H, O**CH**$_2$N), 3.84 (s, 3H, OCH_3), 3.66 (s, 3H, OCH_3), 3.61 (s, 6H, 2OCH_3). ^{13}C-NMR (101 MHz, DMSO-d_6) δ: 166.89, 165.85, 164.73, 162.43, 153.85, 153.02, 138.53, 134.49, 130.31, 129.86, 127.83, 127.00, 126.48, 126.36, 125.75, 125.30, 122.52, 121.12, 114.06, 113.86, 107.77, 107.60, 106.16, 66.92, 60.51, 56.06, 55.89. MS (*m*/*z*, %): 585.59 (M^+, 14.76), 93.44 (100). Analysis: calc. for $C_{32}H_{31}N_3O_8$ (585.61): C 65.63, H 5.34, N 7.18%, found: C 65.43, H 5.52, N 7.36%.

*4.1.1.11. (Z)-N-(1-(Furan-2-yl)-3-(2-(2-(naphthalen-1-yloxy) acetyl)hydrazineyl)-3-oxoprop-1-en-2-yl)benzamide (**6a**).* Pale yellow solid, yield 83%; mp: 234–236 °C. ^{1}H-NMR (400 MHz, DMSO-d_6) δ: 10.34 (s, 1H, NH), 10.24 (s, 1H, NH), 9.89 (s, 1H, NH), 8.38–8.33 (m, 1H), 8.08–8.04 (m, 2H), 7.90–7.87 (m, 1H), 7.78 (d, J = 1.8 Hz, 1H), 7.63–7.58 (m, 2H), 7.55 (d, J = 1.7 Hz, 1H), 7.54–7.53 (m, 2H), 7.52–7.51 (m, 1H), 7.43 (d, J = 8.0 Hz,

1H), 7.24 (s, 1H, $H_{C=C}$), 6.99 (t, J = 6.6 Hz, 1H), 6.76 (d, J = 3.5 Hz, 1H), 6.60 (dd, J = 3.5, 1.8 Hz, 1H), 4.83 (s, 2H, OCH_2N). ^{13}C-NMR (101 MHz, DMSO-d_6) δ: 167.06, 166.25, 164.21, 153.81, 150.00, 145.30, 134.49, 134.31, 132.09, 128.72, 128.43, 127.82, 127.01, 126.47, 126.22, 125.76, 125.29, 122.52, 121.15, 119.13, 114.96, 112.82, 106.14, 66.86. MS (m/z, %): 455.83 (M^+, 36.14), 81.27 (100). Analysis: calc. for $C_{26}H_{21}N_3O_5$ (455.47): C 68.56, H 4.65, N 9.23%, found: C 68.74, H 4.51, N 9.38%.

*4.1.1.12. (Z)-N-(1-(Furan-2-yl)-3-(2-(2-(naphthalen-1-yloxy) acetyl)hydrazineyl)-3-oxoprop-1-en-2-yl)-4-methoxybenzamide (**6b**).* Pale yellow solid, yield 87%; mp: 242–244 °C. ^{1}H-NMR (400 MHz, DMSO-d_6) δ: 10.35 (s, 1H, NH, NH), 9.77 (s, 1H, NH, NH), 9.57 (s, 1H, NH, NH), 8.38 (dd, J = 11.6, 5.7 Hz, 1H), 8.12–8.01 (m, 2H), 7.89 (dd, J = 7.2, 3.5 Hz, 1H), 7.78 (d, J = 4.5 Hz, 1H), 7.55 (dt, J = 9.1, 4.1 Hz, 3H), 7.45–7.40 (m, 1H), 7.22 (d, J = 4.3 Hz, 1H, $H_{C=C}$), 7.08 (d, J = 8.4 Hz, 2H), 7.00 (d, J = 6.9 Hz, 1H), 6.74 (t, J = 4.1 Hz, 1H), 6.65–6.55 (m, 1H), 4.94–4.81 (m, 2H, OCH_2N), 3.86 (s, 3H, OCH_3). ^{13}C-NMR (101 MHz, DMSO-d_6) δ: 167.07, 166.94, 165.67, 164.26, 162.42, 153.85, 150.13, 145.08, 134.50, 130.37, 127.83, 127.00, 126.47, 125.75, 125.30, 122.53, 121.13, 118.66, 114.58, 113.96, 112.80, 106.14, 105.94, 66.92, 55.89. MS (m/z, %): 485.82 (M^+, 46.32), 319.23 (100). Analysis: calc. for $C_{27}H_{23}N_3O_6$ (485.50): C 66.80, H 4.78, N 8.66%, found: C 67.04, H 4.89, N 8.51%.

4.2. Biological activity

The biological evaluation of the constructed naphthalen-1-yloxyacetamide-tethered acrylamide derivatives **5a–j** and **6a**, **6b** was applied as presented in the SI.

Conflicts of interest

The authors have declared no conflict of interest.

Data availability

The authors confirm that the data supporting the findings of this study are available within the article and/or its supporting information (SI). Supplementary information is available. See DOI: **https://doi.org/10.1039/d5ra06524k**.

Acknowledgements

The authors extend their appreciation to Princess Nourah bint Abdulrahman University Researchers Supporting Project number (PNURSP2025R155), Princess Nourah bint Abdulrahman University, Riyadh, Saudi Arabia.

References

1 A. N. Giaquinto, H. Sung, L. A. Newman, R. A. Freedman, R. A. Smith, J. Star, A. Jemal and R. L. Siegel, Breast cancer statistics 2024, *Ca-Cancer J. Clin.*, 2024, **74**, 477–495.

2 J. Kim, A. Harper, V. McCormack, H. Sung, N. Houssami, E. Morgan, M. Mutebi, G. Garvey, I. Soerjomataram and M. M. Fidler-Benaoudia, Global patterns and trends in breast cancer incidence and mortality across 185 countries, *Nat. Med.*, 2025, **31**, 1154–1162.

3 C. Taylor, P. McGale, J. Probert, J. Broggio, J. Charman, S. C. Darby, A. J. Kerr, T. Whelan, D. J. Cutter and G. Mannu, Breast cancer mortality in 500 000 women with early invasive breast cancer diagnosed in England, 1993-2015: population based observational cohort study, *BMJ*, 2023, **381**, e074684.

4 M. Salah hamed Mohamed, A. Mahmoud, H. T. A. A. Rashdan and E. A. M. Mousa, Corneal changes in estrogen-dependent breast cancer after hormonal treatment, *Sci. Rep.*, 2025, **15**, 30330–30335.

5 J. Yao, Y. Tao, Z. Hu, J. Li, Z. Xue, Y. Zhang and Y. Lei, Optimization of small molecule degraders and antagonists for targeting estrogen receptor based on breast cancer: current status and future, *Front. Pharmacol*, 2023, **14**, 1225951–1225973.

6 A. R. Bucknam, J. M. Nicholson, H. S. Radomska, G. M. Young, C. C. Coss and G. C. Micalizio, An Estrogen Receptor β Agonist with AR Antagonist Activity from a Modern Asymmetric De Novo Steroid Synthesis, *ACS Med. Chem. Lett.*, 2025, **16**, 631–637.

7 N. Bhatia and S. Thareja, Aromatase inhibitors for the treatment of breast cancer: An overview (2019–2023), *Bioorg. Chem.*, 2024, **151**, 107607.

8 C. Amaral, C. F. Almeida, M. J. Valente, C. L. Varela, S. C. Costa, F. M. F. Roleira, E. Tavares-da-Silva, A. M. Vinggaard, N. Teixeira and G. Correia-da-Silva, New Promising Steroidal Aromatase Inhibitors with Multi-Target Action on Estrogen and Androgen Receptors for Breast Cancer Treatment, *Cancers*, 2025, **17**, 165.

9 D. Ghosh, J. Griswold, M. Erman and W. Pangborn, Structural basis for androgen specificity and oestrogen synthesis in human aromatase, *Nature*, 2009, **457**, 219–223.

10 V. Müller, M. Hörner, M. Thill, M. Banys-Paluchowski, S. Schmatloch, P. A. Fasching, N. Harbeck, D. Langanke, S. Uhrig, L. Häberle, D. Fischer, A. Hein, T. N. Fehm, C. Goossens, J. Terhaag, U. Heilenkötter, P. Dall, C. Rudlowski, R. Wuerstlein, M. Aydogdu, M.-D. Keyver-Paik, C. Hammerle, N. Deuerling, E. Stickeler, B. Aktas, E. Belleville, M. Thoma, N. Ditsch, Y. Baila, C. Roos, C. Mann, C. Iuliano, S. Y. Brucker, A. Schneeweiss and A. D. Hartkopf, Real-world utilization of aromatase inhibitors, tamoxifen, and ovarian function suppression in premenopausal patients with early hormone receptor-positive, HER2-negative breast cancer with increased recurrence risk, *Breast*, 2025, **81**, 104458.

11 B. Cerra and A. Gioiello, Discovery and development of steroidal enzyme inhibitors as anti-cancer drugs: state-of-the-art and future perspectives, *J. Enzyme Inhib. Med. Chem.*, 2025, **40**, 2483818–2483839.

12 S. Janowska, S. Holota, R. Lesyk and M. Wujec, Aromatase Inhibitors as a Promising Direction for the Search for New Anticancer Drugs, *Molecules*, 2024, **29**, 346–373.

13 Y.-Y. Wu, Q.-L. Huang, Z.-Y. Luo, X.-Y. Song, Y.-Y. Shi, J.-Z. Zheng and S. Liu, Evaluation of dermatologic adverse

events associated with aromatase inhibitors: insights from the FAERS database, *Front. Pharmacol.*, 2025, **16**, 1–10.

14 F. Jin, F. Peng, W.-R. Li, J.-Q. Chai, M. Chen, A.-M. Lu, C.-L. Yang and M.-G. Zhou, Design, synthesis, and antifungal activity of novel cyanoacrylate derivatives containing a naphthalene moiety as potential myosin-5 inhibitor, *J. Saudi Chem. Soc.*, 2024, **28**, 101928.

15 M. M. Edim, O. C. Enudi, B. B. Asuquo, H. Louis, E. A. Bisong, J. A. Agwupuye, A. G. Chioma, J. O. Odey, I. Joseph and F. I. Bassey, Aromaticity indices, electronic structural properties, and fuzzy atomic space investigations of naphthalene and its aza-derivatives, *Heliyon*, 2021, **7**, e06138.

16 A. Elkamhawy, U. M. Ammar, M. Kim, A. R. Gul, T. J. Park and K. Lee, Discovery of novel naphthalene-based diarylamides as pan-Raf kinase inhibitors with promising anti-melanoma activity: rational design, synthesis, in vitro and in silico screening, *Arch. Pharmacal Res.*, 2025, **48**, 150–165.

17 T. Zhu, X. Cui, W. Ma, X. Qi and H. Wei, Synthesis of naphthalene derivatives via nitrogen-to-carbon transmutation of isoquinolines, *Sci. Adv.*, 2025, **11**, eads5928.

18 Y. Cheng, T. T. Yu, E. M. Olzomer, M. Beretta, A. Katen, J. Su, J. P. Jones, D. S. Black, K. L. Hoehn and F. L. Byrne, Design, synthesis and biological evaluation of naphthalene-1, 4-dione analogues as anticancer agents, *RSC Med. Chem.*, 2025, **16**, 2677–2696.

19 D. Selavaraj, K. Vishwanathan, G. Byran, M. Mohan and K. Lakshmanan, Synthesis, Characterization, Docking Studies, and In-vitro Cytotoxic Activity of Some Novel 2, 3 Disubstituted Naphthalene 1, 4 Dione Derivatives, *Curr. Bioact. Compd.*, 2025, **21**, E160424228935.

20 X.-M. Li, Q.-L. Mi, Q. Gao, J. Li, C.-M. Song, W.-L. Zeng, H.-Y. Xiang, X. Liu, J.-H. Chen, C.-M. Zhang, G.-Y. Yang, Q.-F. Hu and Z.-Y. Chen, Antibacterial Naphthalene Derivatives from the Fermentation Products of the Endophytic Fungus Phomopsis fukushii, *Chem. Nat. Compd.*, 2021, **57**, 293–296.

21 Y. Ge, C. Zhang, Y. Qu, L. Ding, X. Zhang, Z. Zhang, C. Jin, X.-N. Wang and Z. Wang, Synthesis and pharmacodynamic evaluation of naphthalene derivatives against influenza A virus in vitro and in vivo, *Eur. J. Med. Chem.*, 2023, **259**, 115660.

22 M. Maheshwari and N. Hussain, Chemical synthesis of substituted naphthalene derivatives: A review, *Synthesis*, 2024, **56**, 2145–2182.

23 A. Aher, P. Bera, P. Brandao, S. Sharda, S. Khatua, S. K. Manna, A. Manhas and P. Bera, Anticancer efficacy of thiazole-naphthyl derivatives targeting DNA: Synthesis, crystal structure, density functional theory, molecular docking, and molecular dynamics studies, *Int. J. Biol. Macromol.*, 2025, **299**, 140039.

24 W. Chen, Y. Shen, Z. Li, M. Zhang, C. Lu and Y. Shen, Design and synthesis of 2-phenylnaphthalenoids as inhibitors of DNA topoisomeraseIIα and antitumor agents, *Eur. J. Med. Chem.*, 2014, **86**, 782–796.

25 A. E. Evren, D. Nuha, S. Dawbaa, B. N. Sağlık and L. Yurttaş, Synthesis of novel thiazolyl hydrazone derivatives as potent dual monoamine oxidase-aromatase inhibitors, *Eur. J. Med. Chem.*, 2022, **229**, 114097.

26 M. E. Salem, E. M. Mahrous, E. A. Ragab, M. S. Nafie and K. M. Dawood, Synthesis of novel mono- and bis-pyrazolylthiazole derivatives as anti-liver cancer agents through EGFR/HER2 target inhibition, *BMC Chem.*, 2023, **17**, 51.

27 G. Wang, W. Liu, Z. Gong, Y. Huang, Y. Li and Z. Peng, Synthesis, biological evaluation, and molecular modelling of new naphthalene-chalcone derivatives as potential anticancer agents on MCF-7 breast cancer cells by targeting tubulin colchicine binding site, *J. Enzyme Inhib. Med. Chem.*, 2020, **35**, 139–144.

28 G. Wang, W. Liu, Z. Peng, Y. Huang, Z. Gong and Y. Li, Design, synthesis, molecular modeling, and biological evaluation of pyrazole-naphthalene derivatives as potential anticancer agents on MCF-7 breast cancer cells by inhibiting tubulin polymerization, *Bioorg. Chem.*, 2020, **103**, 104141.

29 R. Leechaisit, R. Pingaew, V. Prachayasittikul, A. Worachartcheewan, S. Prachayasittikul, S. Ruchirawat and V. Prachayasittikul, Synthesis, molecular docking, and QSAR study of bis-sulfonamide derivatives as potential aromatase inhibitors, *Bioorg. Med. Chem.*, 2019, **27**, 115040.

30 H. M. Abd El-Lateef, T. H. Alharbi, E. Fayad, H. A. Katouah, F. G. Elsaid, M. Alsunbul, W. S. Al-Qahtani, A. H. Abu Almaaty, A. G. Ahmed Gaafar and M. I. Salama, Novel quinolin-4-ylcarbonylhydrazine having N-(3-arylacryloyl) moiety: Design, synthesis and biological evaluation as potential cytotoxic agents against MDA-MB-231 via tubulin assembly inhibition, *J. Mol. Struct.*, 2025, **1321**, 140214.

31 M. A. Alghamdi, M. R. Abdulbaqi, D. S. Alshaya, J. Alharthi, H. A. Katouah, F. G. Elsaid, E. Fayad, A. H. A. Almaaty, A. Y. A. Alzahrani and B. Y. Beshay, Design, synthesis and cytotoxic research of a novel antitumor model based on acrylamide–PABA analogs via β-tubulin inhibition, *RSC Adv.*, 2025, **15**, 18490–18500.

32 F. Yu, L. Chi, H. Wang, C. Gao, H. Dai, L. Liu, Z. Wang, Y. Ke, H. Liu and Q. Zhang, Design, synthesis and antitumor activity evaluation of 5-cyano-2,4,6-substituted pyrimidine derivatives containing acrylamide group, *Med. Chem. Res.*, 2023, **32**, 2116–2124.

33 D. Grenier, S. Audebert, J. Preto, J.-F. Guichou and I. Krimm, Linkers in fragment-based drug design: an overview of the literature, *Expert Opin. Drug Discovery*, 2023, **18**, 987–1009.

34 N. Yadav, K. Kumar, V. Singh, S. Rai, K. Blahatia, A. Das and T. Jana, Newly designed acrylamide derivative-based pH-responsive hydrogel-urease bioconjugates: synthesis and catalytic urea hydrolysis, *Soft Matter*, 2022, **18**, 8647–8655.

35 B. Goel, S. Jaiswal and S. K. Jain, Indole derivatives targeting colchicine binding site as potential anticancer agents, *Arch. Pharm.*, 2023, **356**, 2300210.

36 H. M. Abd El-Lateef, D. Bafail, N. H. Y. Alhalees, E. E. Toson, A. H. A. Almaaty, E. H. Elsayed, I. Zaki and M. M. Youssef, Synthesis, characterization and biological research of novel

2-(quinoline-4-carbonyl) hydrazide-acrylamide hybrids as potential anticancer agents on MCF-7 breast carcinoma cells by targeting EGFR-TK, *RSC Adv.*, 2024, **14**, 23495–23504.

37 C. Tan, S. Li, J. Song, X. Zheng, H. Zheng, W. Xu, C. Wan, T. Zhang, Q. Bian and S. Men, 3,4-Dichlorophenylacetic acid acts as an auxin analog and induces beneficial effects in various crops, *Commun. Biol.*, 2024, **7**, 161.

38 L. M. A. A. Ghany, N. Ryad, M. S. Abdel-Aziz, H. M. A. El-Lateef, I. Zaki and B. Y. Beshay, Design, synthesis, antimicrobial evaluation, and molecular modeling of new sulfamethoxazole and trimethoprim analogs as potential DHPS/DHFR inhibitors, *J. Mol. Struct.*, 2024, **1309**, 138170.

39 H. M. Abd El-Lateef, E. E. M. Toson, A. H. Abu Almaaty, R. M. Saleem, A. H. A. Maghrabi, E. H. El-Sayed, I. Zaki and M. M. Youssef, Synthesis, Characterization and Biological Evaluation of New Enamide Fluorinated-Schiff Base Derivatives as Potential Cytotoxic and Apoptosis-Inducing Agents, *ChemistrySelect*, 2023, **8**, e202303070.

40 T. Al-Warhi, A. Aldhahrani, F. Althobaiti, E. Fayad, O. A. Abu Ali, S. Albogami, A. H. Abu Almaaty, A. I. M. Khedr, S. N. A. Bukhari and I. Zaki, Design, Synthesis and Cytotoxic Activity Evaluation of Newly Synthesized Amides-Based TMP Moiety as Potential Anticancer Agents over HepG2 Cells, *Molecules*, 2022, **27**, 3960.

41 B. Cerra and A. Gioiello, Discovery and development of steroidal enzyme inhibitors as anti-cancer drugs: state-of-the-art and future perspectives, *J. Enzyme Inhib. Med. Chem.*, 2025, **40**, 2483818.

42 L. Xin, C. Wang, Y. Cheng, H. Wang, X. Guo, X. Deng, X. Deng, B. Xie, H. Hu, C. Min, C. Dong and H.-B. Zhou, Discovery of Novel ERα and Aromatase Dual-Targeting PROTAC Degraders to Overcome Endocrine-Resistant Breast Cancer, *J. Med. Chem.*, 2024, **67**, 8913–8931.

43 B. Crespo, J. C. Illera, G. Silvan, P. Lopez-Plaza, M. Herrera de la Muela, M. de la Puente Yagüe, C. Diaz del Arco, M. J. Illera and S. Caceres, Androgen and Estrogen β Receptor Expression Enhances Efficacy of Antihormonal Treatments in Triple-Negative Breast Cancer Cell Lines, *Int. J. Mol. Sci.*, 2024, **25**, 1471.

44 P. Ryszkiewicz, B. Malinowska and E. Schlicker, Polypharmacology: new drugs in 2023–2024, *Pharmacol. Rep.*, 2025, **77**, 543–560.

45 K. M. Ismail, S. S. Hassan and D. H. Hanna, Palladium-Imidazole Nanoparticles' Cytotoxic Effects on Colon Cancer Cells: Induction of Cell Cycle Arrest and Apoptosis Mediated via Mitochondria, *Appl. Organomet. Chem.*, 2025, **39**, e7908.

46 B. Sui, R. Wang, C. Chen, X. Kou, D. Wu, Y. Fu, F. Lei, Y. Wang, Y. Liu, X. Chen, H. Xu, Y. Liu, J. Kang, H. Liu, R. T. K. Kwok, B. Z. Tang, H. Yan, M. Wang, L. Xiang, X. Yan, X. Zhang, L. Ma, S. Shi and Y. Jin, Apoptotic Vesicular Metabolism Contributes to Organelle Assembly and Safeguards Liver Homeostasis and Regeneration, *Gastroenterology*, 2024, **167**, 343–356.

47 A. Tkachenko, Apoptosis and eryptosis: similarities and differences, *Apoptosis*, 2024, **29**, 482–502.

48 H. H. Kim, S.-Y. Lee and D.-H. Lee, Apoptosis of Pancreatic Cancer Cells after Co-Treatment with Eugenol and Tumor Necrosis Factor-Related Apoptosis-Inducing Ligand, *Cancers*, 2024, **16**, 3092.

49 C.-J. Zuo and J. Tian, Advancing the understanding of the role of apoptosis in lung cancer immunotherapy: Global research trends, key themes, and emerging frontiers, *Hum. Vaccines Immunother.*, 2025, **21**, 2488074.

50 I. Zaki, M. K. Abdelhameid, I. M. El-Deen, A. H. A. Abdel Wahab, A. M. Ashmawy and K. O. Mohamed, Design, synthesis and screening of 1, 2, 4-triazinone derivatives as potential antitumor agents with apoptosis inducing activity on MCF-7 breast cancer cell line, *Eur. J. Med. Chem.*, 2018, **156**, 563–579.

51 V. Shoshan-Barmatz, T. Arif and A. Shteinfer-Kuzmine, Apoptotic proteins with non-apoptotic activity: expression and function in cancer, *Apoptosis*, 2023, **28**, 730–753.

52 D. Yilmaz, M. Gürsoy and U. K. Gürsoy, Anti-Apoptotic and Pro-Apoptotic Bcl-2 Family Proteins in Peri-Implant Diseases, *Clin. Oral Implants Res.*, 2023, **34**, 582–590.

53 Z. Zhou, T. Arroum, X. Luo, R. Kang, Y. J. Lee, D. Tang, M. Hüttemann and X. Song, Diverse functions of cytochrome c in cell death and disease, *Cell Death Differ.*, 2024, **31**, 387–404.

54 P. Mystek, V. Singh, M. Horváth, K. Honzejková, P. Riegerová, H. Evci, M. Hof, T. Obšil and R. Šachl, The minimal membrane requirements for BAX-induced pore opening upon exposure to oxidative stress, *Biophys. J.*, 2024, **123**, 3519–3532.

55 M. A. McDonnell, D. Wang, S. M. Khan, M. G. Vander Heiden and A. Kelekar, Caspase-9 is activated in a cytochrome c-independent manner early during TNFα-induced apoptosis in murine cells, *Cell Death Differ.*, 2003, **10**, 1005–1015.

56 K. Aral, C. A. Aral and Y. Kapila, The role of caspase-8, caspase-9, and apoptosis inducing factor in periodontal disease, *J. Periodontol.*, 2019, **90**, 288–294.

57 S. Kasana, S. Kumar, P. Patel, B. D. Kurmi, S. Jain, S. Sahu and A. Vaidya, Caspase inhibitors: a review on recently patented compounds (2016–2023), *Expert Opin. Ther. Pat.*, 2024, **34**, 1047–1072.

58 K. Matsui, M. Watanabe, S. Yamamoto, S. Kawagoe, T. Ikeda, H. Ohashi, T. Kuroda, N. Koda, K. Morimoto, Y. Kinoshita, Y. Inage, Y. Saito, S. Fukunaga, T. Fujimoto, S. Tajiri, K. Matsumoto, E. Kobayashi, T. Yokoo and S. Yamanaka, Caspase 9-induced apoptosis enables efficient fetal cell ablation and disease modeling, *Nat. Commun.*, 2025, **16**, 2572.